ISSN 1023-1935, Russian Journal of Electrochemistry, 2006, Vol. 42, No. 10, pp. 1055–1060. © MAIK "Nauka/Interperiodica" (Russia), 2006.
Published in Russian in Elektrokhimiya, 2006, Vol. 42, No. 10, pp. 1173–1179.

Electrocatalytic Activity of Sol–Gel-Prepared RuO_2/Ti Anode in Chlorine and Oxygen Evolution Reactions*

V. V. Panić,[a,z] A. B. Dekanski,[a] S. K. Milonjić,[b] V. B. Mišković-Stanković,[c] and B. Ž. Nikolić[c]

[a] *Institute of Chemistry, Technology, and Metallurgy, Njegoševa 12, 11000 Belgrade, Serbia and Montenegro*
[b] *Vinča Institute of Nuclear Sciences, P.O.B. 522, 11001 Belgrade, Serbia and Montenegro*
[c] *University of Belgrade, Karnegijeva 4, 11000 Belgrade, Serbia and Montenegro*

Received March 22, 2006

Abstract—Electrocatalytic properties of RuO_2/Ti anode with different coating masses, which are prepared by the alkoxide sol–gel procedure, are investigated in chlorine and oxygen evolution reactions by polarization measurements and electrochemical impedance spectroscopy in H_2SO_4 and NaCl electrolytes. According to polarization measurements, the activity of anodes at overpotentials below 100 mV is independent of coating mass. However, impedance measurements above 100 mV reveal changes in the activity of anodes in chlorine evolution reaction for different coating masses. The diffusion limitations related to the evolved chlorine are registered in low-frequency domain at 1.10 V (SCE), diminishing with the increase in potential to the 1.15 V (SCE). The observed impedance behavior is discussed with respect to the activity model for activated titanium anodes in chlorine evolution reaction involving formation of gas channels within porous coating structure. Gas channels enhance the mass transfer rate similarly to the forced convection, which also increases the activity of anode. This is more pronounced for the anode of greater coating mass due to its more compact surface structure. The more compact structure appears to be beneficial for gas channels formation.

DOI: 10.1134/S1023193506100107

Key words: electrocatalysis, RuO_2/Ti anode, chlorine evolution, oxygen evolution, sol–gel method

INTRODUCTION

Due to considerable electrocatalytic activity in the chlorine evolution reaction (CER), ruthenium-oxide-based electroactive coatings on titanium substrate are used as anodes for industrial production of chlorine [1] and chlorates [2]. The coatings are of good catalytic properties for many other electrochemical processes [3]. They have also excellent capacitive characteristics owing to the pseudocapacitive behavior [4], which makes them applicable in the field of electrochemical supercapacitors [5, 6].

The properties of ruthenium oxide and electrochemical behavior of anodic oxide coatings depend on oxide preparation procedure and the method of coating formation. Electrocatalytic properties and stability of activated titanium anodes can be significantly improved if the active coating is prepared by a sol–gel procedure [7, 8], as an alternative to the commonly used preparation procedure that involves thermal decomposition of metal chlorides [1, 3]. Improvement of the properties of activated titanium anodes, obtained by the sol–gel procedure from oxide colloidal dispersions prepared by forced hydrolysis of metal chlorides in acid solution, was assigned to the homogeneous distribution of fine oxide particles, i.e. to the larger real surface area of such a coating in comparison to that obtained by thermal decomposition [9].

Investigations of CER kinetics on activated titanium anodes showed that the reaction is extremely fast, being activationless at lower overpotentials [10, 11]. Proposed mechanism consists of the following elementary steps [12]:

$$Cl^- \rightleftharpoons Cl_{ads} + e \quad (1)$$

$$Cl_{ads} \longrightarrow Cl^+ + e \quad (2)$$

$$Cl^+ + Cl^- \rightleftharpoons Cl_2. \quad (3)$$

Kinetics and transport phenomena of CER were also investigated by electrochemical impedance spectroscopy (EIS) in particular [12]. Li et al. [13] investigated CER on Pt by EIS and proposed that the CER mechanism on Pt consists of two elementary steps, in which adsorption step (1) is followed by recombination:

$$2Cl_{ads} \longrightarrow Cl_2. \quad (4)$$

Complex-plane diagrams are characterized by the appearance of the faradaic impedance at high frequencies followed by Warburg impedance at low frequencies [13], which is due to diffusion of evolved chlorine from the electrode surface towards the electrolyte bulk. The Warburg impedance disappears under forced con-

* The text was submitted by the authors in English.
[z] Corresponding author, email: panic@ihtm.bg.ac.yu

vection conditions, and three separate semicircles rise in complex-plane plot. Considering connection between the charge transfer resistance and CER kinetic parameters according to the mechanism containing steps (1) and (4), Li et al. [13] ascribed the high-frequency semicircle to the charge transfer in step (1), while the semicircle at medium frequencies corresponds to step (4). These authors ascribed the semicircle in low-frequency domain to the formation of Pt–O bound, since its characteristics depend on the electrode state before CER.

Ruthenium oxide is also one of the most active electrocatalysts for the oxygen evolution reaction (OER), since the overpotentials are almost half of that registered on Pt [14, 15]. The Tafel slope increases from 40 mV at low overpotentials to 120 mV at higher overpotentials [16]. At low overpotentials, OER mechanism can be as follows [16]:

$$RuO_2 + H_2O \longrightarrow RuO_2\text{–}OH + H^+ + e \quad (5)$$

$$RuO_2\text{–}OH \rightleftharpoons RuO_3 + H^+ + e \quad (6)$$

$$2RuO_3 \rightleftharpoons 2RuO_2 + O_2. \quad (7)$$

It is assumed that side reaction of ruthenium oxide electrochemical dissolution starts at higher overpotentials, which causes an increase in the Tafel slope. Two parallel reactions of oxygen evolution and ruthenium oxide dissolution appear to have the same rate-determining step. In the latter case, the following elementary steps take place instead of reaction (7):

$$RuO_3 + H_2O \rightleftharpoons RuO_3\text{–}OH + H^+ + e \quad (8)$$

$$RuO_3\text{–}OH \rightleftharpoons RuO_4 + H^+ + e. \quad (9)$$

These reactions are the main cause for limited stability of activated titanium anodes during prolonged electrolysis of diluted chloride solutions.

Having in mind the advantages of sol–gel preparation procedure in comparison to thermal decomposition of metal chlorides, the aim of this work is to prepare RuO_2/Ti anode from ruthenium ethoxide in order to simplify the procedure of coating deposition, and to investigate the properties of obtained anodes for CER and OER.

EXPERIMENTAL

Hydrous ruthenium oxide was prepared from $RuCl_3$ dissolved in ethanol [7, 17]. Prior to the dissolution, commercial $RuCl_3 \cdot xH_2O$ was dried at a temperature of 110°C in nitrogen atmosphere for 24 hours. After the rise of the solution temperature to the boiling point (~76°C) under the reflux condition in nitrogen atmosphere, 20 wt % ethanol solution of sodium ethoxide, NaOEt, was slowly added into the boiling solution in the amount that will give 0.10 M $Ru(OEt)_3$. Formed ethoxide was then left under mixing to hydrolyze for an hour without addition of any hydrolyzing agent as in [7].

The obtained precipitate was separated from the solution and rinsed with distilled water, in order to separate RuO_2 from NaCl. After the drying in air at 120°C for 24 hours, hydrous oxide was suspended in ethanol by using an ultrasonic bath (70 kHz). The suspension became satisfactorily stable (during the period needed for anode preparation) after 45 minutes of ultrasonic treatment. Prepared suspension was used for anode formation.

Titanium rods (3 mm) were used as a support for active RuO_2 coating. The rods were degreased in NaOH-saturated ethanol solution, etched in hot HCI solution and dipped in oxide suspension. The formed layer was then dried at 70°C. The dipping and drying were repeated until the coating weight of 0.61 or 1.1 mg cm^{-2} was reached. The final step in the RuO_2/Ti anode formation was the calcination at a temperature of 450°C for an hour.

Surface appearance of prepared anodes was checked by scanning electron microscopy (SEM), using a JEOL microscope, Model JSM-T20 (U_w = 20 kV).

The anode activity in CER and OER was investigated by potentiodynamic (0.50 mV s^{-1}) polarization measurements in 5 M NaCl (pH 2) and 1.0 M H_2SO_4 solutions. The EIS measurements in the same solutions were carried out using sinusoidal voltage of the amplitude of 10 mV, around the potentials of 1.10, 1.13 and 1.15 V (CER) or 1.15 and 1.25 V (OER). The experiments were conducted at room temperature (~25°C) in a cell equipped with a Pt-mesh counter electrode and a saturated calomel electrode (SCE) with working electrode surface area of 1.2 cm^2. All potentials are referred to the SCE scale.

RESULTS AND DISCUSSION

Polarization curves for CER on prepared RuO_2/Ti anode with different coating masses are shown in Fig. 1. Tafel slope close to 30 mV was registered, which corresponds to the mechanism given by reactions (1) to (3) in the region of relatively low overpotentials. The slope is independent of the coating mass, while the activity of the anode with a thicker coating is somewhat higher at 1.00–1.05 and above 1.075 V. Since CER is an extremely fast process (with high exchange current density), the activity in CER is similar to that at low overpotentials for different mass of active material. This was also registered earlier [18], when freshly prepared and deactivated (after prolonged electrolysis of diluted chloride solution) Ti/RuO_2–TiO_2 anodes showed similar activity in CER, despite considerable decrease in active material concentration in deactivated anode coating. According to the theory and model of porous electrodes [19, 20], small difference in activity at potentials above 1.075 V appears to be closely related to the difference in morphology of coatings that are of different thickness. Some SEM micrographs of prepared anodes are shown in Fig. 2. Both thin and thick

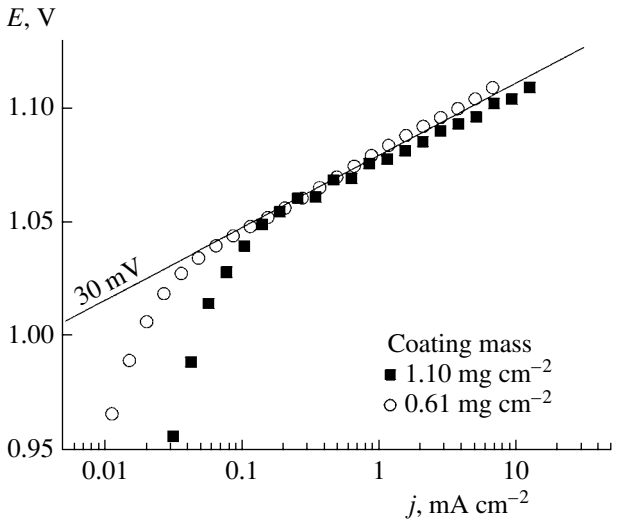

Fig. 1. Tafel plots for RuO_2/Ti anode, prepared by alkoxide sol–gel procedure with different coating masses, registered in 5 M NaCl (pH 2) at room temperature.

coating are of cracked-mud structure, while the islands of thick coating (Fig. 2b) are of considerably more compact surface than the islands of thin coating (Fig. 2a). As the consequence of such surface appearance, one should expect larger extent of narrow pores in thick coating, although they are not seen in Fig. 2b.

Comparing the polarization characteristics given in Fig. 1 to our earlier results, it follows that anodes prepared by the alkoxide sol–gel procedure are more active in CER and OER than those obtained from oxide sols prepared by forced hydrolysis of metal chlorides [21, 22]. The current densities measured in CER for the anodes prepared by the alkoxide sol–gel procedure are about twice those for RuO_2/Ti anodes prepared from oxide sols synthesized by forced hydrolysis of $RuCl_3$ [22]. However, if current densities are normalized to electrochemically active surface area [23] obtained by cyclic voltammetry measurements, differently prepared anodes show quite similar activity in CER. This means that difference in measured polarization data is due to the difference in real surface area and, consequently, that RuO_2 coatings prepared by different sol–gel procedures are of similar physicochemical properties (crystalline state, lattice parameters, hydration degree), so that the difference in activity can be ascribed to different morphology.

Polarization curves for OER on prepared RuO_2/Ti anode with different coating masses are shown in Fig. 3. The Tafel slope is close to 40 mV, which is a typical value for OER on this type of anodes. The anode activity in OER is independent of the coating mass.

More detailed insight into the activity of prepared anodes can be obtained from EIS measurements, especially in the case of CER. Figure 4 shows complex-plane plots for prepared anodes, registered in 5 M NaCl (pH 2) at a potential of 1.10 V. The plots indicate pro-

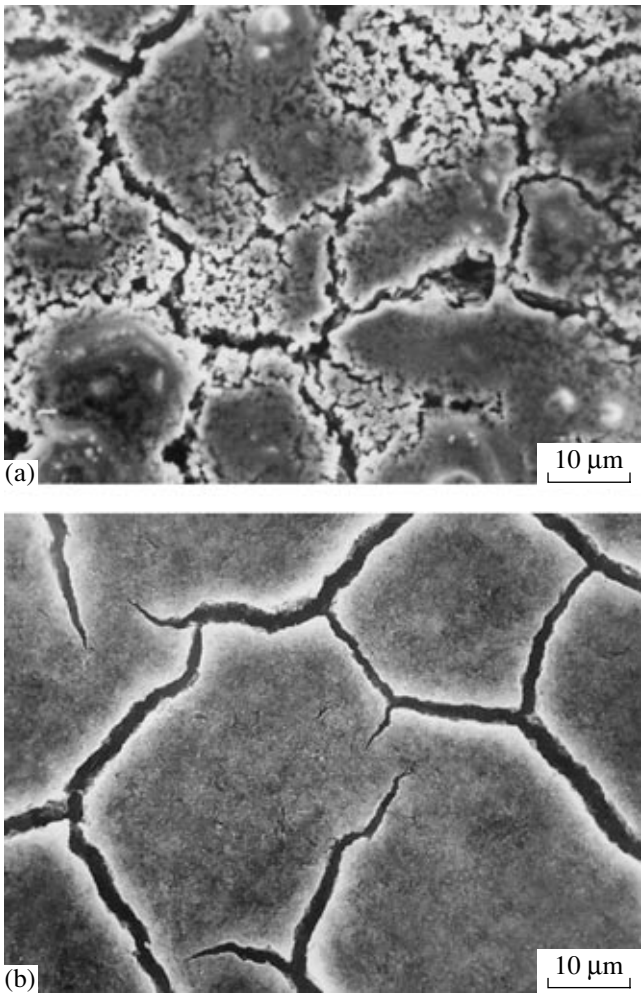

Fig. 2. SEM micrographs of RuO_2/Ti anodes prepared by alkoxide sol–gel procedure with coating masses of (a) 0.61 and (b) 1.10 mg cm^{-2}.

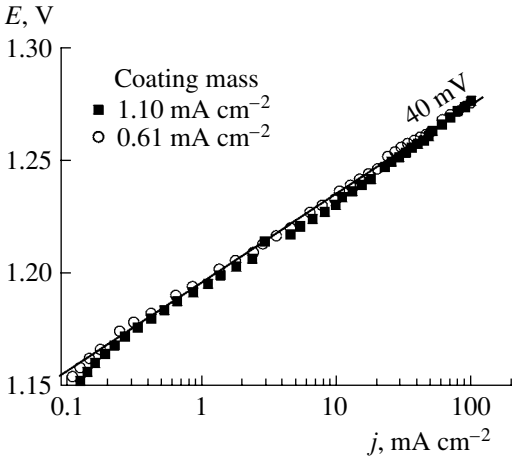

Fig. 3. Tafel plots for RuO_2/Ti anode, prepared by alkoxide sol–gel procedure with different coating masses, registered in 1.0 M H_2SO_4 at room temperature.

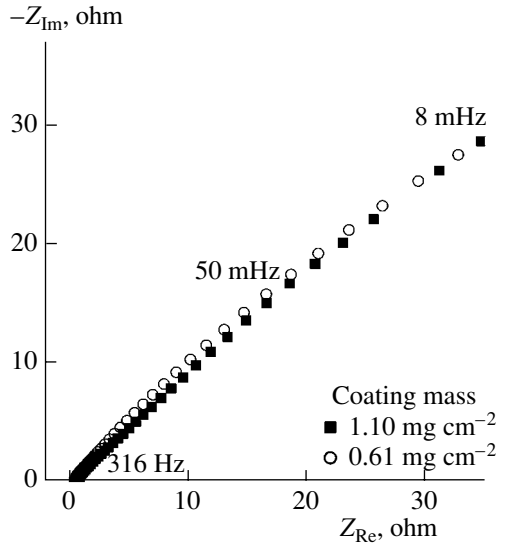

Fig. 4. Complex-plane plots for RuO_2/Ti anode, prepared by alkoxide sol–gel procedure with different coating masses, registered in 5 M NaCl (pH 2) at 1.10 V.

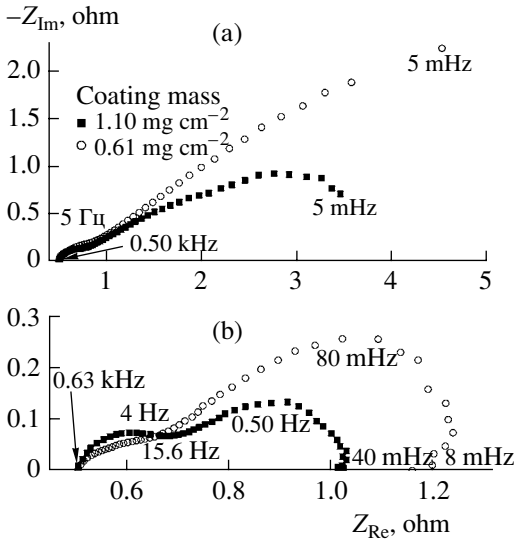

Fig. 5. Same as in Fig. 4, at (a) 1.13 and (b) 1.15 V.

nounced diffusion limitations for CER, since they are almost linear, with a slope of 45°, which is an intrinsic property of classic Warburg impedance. This means that CER is controlled by chlorine diffusion away from outer coating surface facing the electrolyte bulk. Consequently, impedance values are quite similar for different coating masses.

At potentials of 1.13 and 1.15 V, semicircles appear at frequencies above 5.0 Hz (Fig. 5). Semicircle diameters are similar for different coating masses, although the semicircle for the thin coating (0.61 mg cm^{-2}) at 1.15 V is considerably depressed. These impedance characteristics indicate that this semicircle corresponds to the charge transfer in fast adsorption step (1).

While high-frequency semicircle is followed by semicircle-like dependencies at lower frequencies (5.0 Hz–5.0 mHz) in the case of thick coating, the data for the thin coating at low frequencies still show characteristics of diffusion-limited process at 1.13 V (Fig. 5a). This kind of diffusion characteristics completely disappears at 1.15 V for both thick and thin coating (Fig. 5b). A well-defined semicircle is seen at low frequencies instead of diffusion-controlled plots, which can be assigned to the charge transfer reaction presented by relation (2). Semicircle diameter is greater for the thin coating.

Two indications, based on Fig. 5, need to be discussed further. The difference in EIS behavior at low frequencies between the coatings of different thickness indicates the influence of quasi-3D coating morphology on chlorine diffusion process, since the kinetics of CER is expected to be the same for different masses of coatings consisting of the same material. Secondly, diffusion characteristics at 1.10 V (Fig. 4) are not the same as those at 1.13 and 1.15 V (Fig. 5), since the latter does not behave as the classic Warburg impedance. This indicates that the diffusion limitations are related to CER's taking place at the inner coating surface defined by the coating's pores.

Namely, according to the model for activated titanium anodes in CER at high overpotentials [20], the electrolyte can access porous structure more easily at high overpotentials, when gas bubbles form intensively, due to formation of so-called gas channels within porous structure [20]. Mass transport can be thus improved owing to the fluctuation and instant penetration of the electrolyte through gas channels, which enhances mass transport similarly to the forced convection. The onset of this forced micro-convection is seen in Fig. 5 as the appearance of a modified Warburg impedance at low frequencies, which involves finite diffusion through the coating pores instead of semi-infinite one seen in Fig. 4. In addition, the model [20] predicts a decrease in the Tafel slope for CER (from 30 to 25 mV) with increasing overpotential due to enhanced mass transport rate.

Since the thick-coating surface is of more compact island surface than thin one (Fig. 2), it is more difficult for evolved gas to leave the pores of thick coating. Consequently, gas channels can form more easily in the bulk of thick coating. The effect of mass transport enhancement is thus seen at lower potential for thick coating than for thin one (Fig. 4), while the impedance for thick coating is considerably lower in the low-frequency domain at the potential where the onset of forced micro-convection is evident (Fig. 5).

Complex-plane plots and Bode module plots of EIS data for RuO_2/Ti anodes, with different coating masses, in 1.0 M H_2SO_4 at 1.15 V, are shown in Fig. 6. The loops

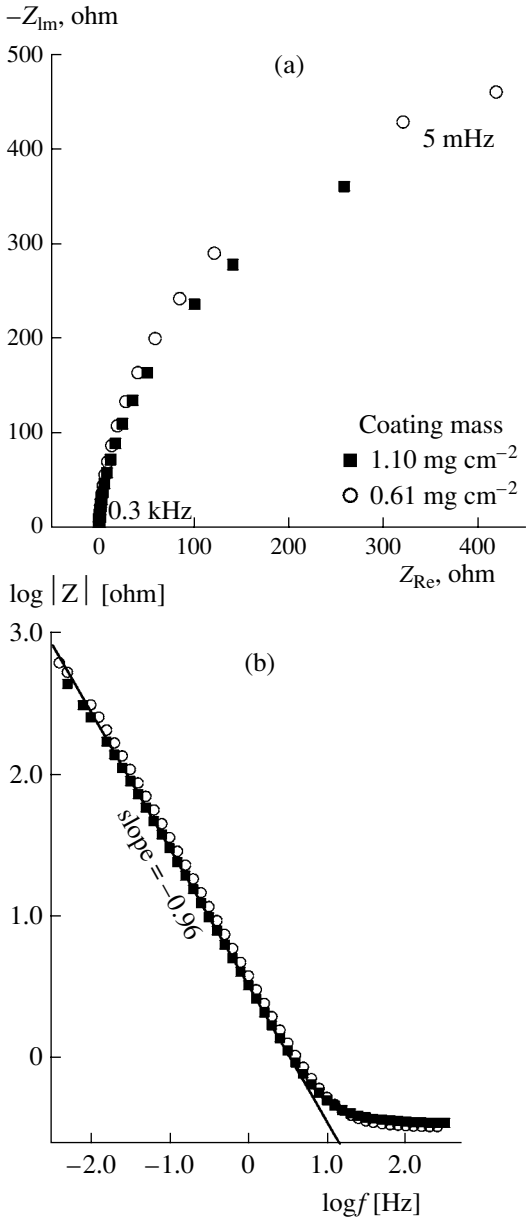

Fig. 6. (a) Complex-plane plots and (b) Bode module plots of EIS data for RuO_2/Ti anodes, prepared by alkoxide sol–gel procedure with different coating masses, registered in 1.0 M H_2SO_4 at 1.15 V.

seen in Fig. 6a can be related to charge transfer. Charge transfer resistances appear to be rather high (~1 kohm). On the other hand, Bode plots (Fig. 6b) at low frequencies approach linear dependences with the slope close to –1, which indicates overall coating capacitive behavior at the applied potential. Owing to high charge transfer resistances and high electrostatic-charge storage ability of RuO_2 [5], a nonfaradaic charging current is considerably higher than the faradaic one when $f \longrightarrow 0$, which causes capacitor-like EIS response seen in Fig. 6b. Since the semicircle for the thick coating is slightly smaller, it appears that the related anode is

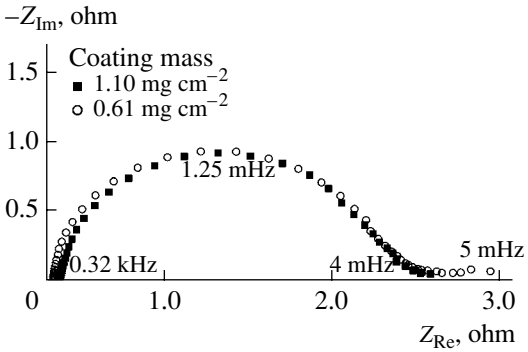

Fig. 7. Complex plane plots of EIS data for RuO_2/Ti anodes, prepared by alkoxide sol–gel procedure with different coating masses, registered in 1.0 M H_2SO_4 at 1.25 V.

more active in OER at the applied potential than the anode with the thin coating.

The activity of prepared anodes in OER at 1.25 V is given in Fig. 7 by means of EIS data. Charge transfer resistance related to OER considerably decreases with respect to the data for 1.15 V (Fig. 6a), while the corresponding semicircles appear completely developed in the frequency range where only loops are seen at 1.15 V. The semicircle diameters associated with the charge transfer resistances are quite similar for different coating masses, indicating coating mass-independent activity in OER, as registered also by polarization measurements (Fig. 3). The charge transfer resistances related to semicircles in Fig. 7 are considerably lower than for RuO_2/Ti–TiO_2 anodes prepared from oxide inorganic colloidal dispersions, for which incompletely developed semicircles were registered in the same electrolyte and at the same potential [18].

Inspecting low-frequency impedance behavior in Fig. 7, the imaginary component in the case of thin coating almost vanishes at higher frequencies if compared to the thick one. Due to larger extent of narrow pores in thick coating, ac modulation has to be of lower frequency to penetrate through thick coating.

CONCLUSIONS

An activated titanium anode, RuO_2/Ti, was prepared by an alkoxide sol–gel procedure. Polarization measurements in chloride solution indicate that the anode activity in the chlorine evolution reaction (CER) is independent of the coating mass at overpotentials reaching 100 mV. A difference in activity was registered by impedance measurements at overpotentials higher than 100 mV. Diffusion limitations due to diffusion of evolved chlorine away from the coating's surface are seen at lower potentials, but these features diminish at higher potentials. This is due to mass transfer enhancement caused by the formation of gas channels within the coating porous structure, which produces a forced micro-convection effect. This effect is

more pronounced in the case of anode of larger coating mass, because it is of more compact surface than the anode with smaller coating mass.

The anode activity in the oxygen evolution reaction is independent of the coating mass, as proved by both polarization and impedance measurements.

The prepared anode appears to be more active in CER than the anode prepared from inorganic oxide colloidal dispersion, owing to the larger real surface area.

ACKNOWLEDGMENTS

This work was supported by the Ministry of Science and Environmental Protection, Republic of Serbia, contract no. 142 061.

REFERENCES

1. Trasatti, S. and O'Grady, W., in *Advances in Electrochemistrey and Electrochemical Engineering*, Gerisher, H. and Tobias, C.W., Eds., New York: Wiley, 1981, vol. 12.
2. Cornell, A. and Herlitz, F., *Proc. 4th Kurt Schwabe Corrosion Symp.,* Helsinki, 2004, p. 326.
3. Trasatti, S., in *Interfacial Electrochemistry: Theory, Experiment, and Applications*, Wieckowski, A., Ed., New York: Marcel Dekker, 1999, p. 769.
4. Jow, T. and Zheng, J., *J. Electrochem. Soc.*, 1998, vol. 145, p. 49.
5. Conway, B.E., *Electrochemical Supercapacitors: Scientific Fundamentals and Technological Applications,* New York: Kluwer Academic/Plenum, 1999.
6. Panić, V., Vidaković, T., Gojković, S., Dekanski, A., Milonjić, S., and Nikolić, B., *Electrochim. Acta*, 2003, vol. 48, p. 3805.
7. Komeyama, K., Shohji, S., Onoue, S., Nishimura, K., Yahikozawa, K., and Takasu, Y., *J. Electrochem. Soc.*, 1993, vol. 140, p. 1034.
8. Paniç, V., Dekanski, A., Milonjić, S., Atanasoski, R., and Nikolić, B., *Colloids Surf. A*, 1999, vol. 157, p. 269.
9. Paniç, V., Dekanski, A., Wang, G., Fedoroff, M., Milonjiç, S., and Nikolić, B., *J. Colloid Interface Sci.,* 2003, vol. 263, p. 68.
10. Krishtalik, L., *Electrochim. Acta*, 1981, vol. 26, p. 329.
11. Krishtalik, L., in *Comprehensive Treatise of Electrochemistry,* Conway, B., Bockris, J.O'M., Yeager, E., Khan, S., and White, R., Eds., New York: Plenum, 1983, vol. 7, p. 87.
12. Christensen, P.A. and Hamnet, A., *Techniques and Mechanisms in Electrochemistry*, New York: Springer, 1994, p. 154.
13. Li, B., Hillman, A.R., and Lubetkin, S.D., *Electrochim. Acta*, 1992, vol. 37, p. 2715.
14. Lodi, G., Sivieri, E., De Battisti, A., and Trasatti, S., *J. Appl. Electrochem.*, 1978, vol. 8, p. 135.
15. Chang, C.C. and Wen, T.C., *J. Appl. Electrochem.*, 1997, vol. 27, p. 355.
16. Gajić-Krstajić, L.M., Trisović, T.L., and Krstajić, N.V., *Corros. Sci.*, 2004, vol. 46, p. 65.
17. Armelao, L., Barreca, D., and Moraru, B., *J. Noncryst. Solids*, 2003, vol. 316, p. 364.
18. Panić, V., Dekanski, A., Miškoviç-Stanković, V.B., Milownjiç, S., and Nikolić, B, *J. Electroanal. Chem.,* 2005, vol. 579, p. 67.
19. Chizmadzev, Yu. and Chirkov, Yu., in *Comprehensive Threatise of Electrochemistry*, Yeager, E., Bockris, J.O'M., Conway, B., and Sarangapani, S., Eds., New York: Plenum, 1983, vol. 6, ch. 5.
20. Evdokimov, S.V., *Russ. J. Electrochem.*, 2000, vol. 36, p. 609.
21. Panić, V., Dekanski, A., Milonjiç, S., Atanasoski, R., and Nikolić, B., *Electrochim. Acta*, 2000, vol. 46, p. 415.
22. Paniç, V., Dekanski, A., Milonjić, S., Atanasoski, R., and Nikoliç, B., *Mater. Sci. Forum,* 2000, vol. 352, p. 117.
23. Mattos-Costa, F.I., de Lima-Neto, P., Machado, S.A.S., and Avaca, L.A., *Electrochim. Acta*, 1998, vol. 44, p. 1515.